Earthquakes and Structures, *Vol. 13, No. 3 (2017) 299-307*
DOI: http://dx.doi.org/10.12989/eas.2017.13.3.299

RTS test study and numerical simulation of mechanical properties of HDR bearings

Tianbo Peng*[1,2] and Yicheng Wu[1,2]

[1]*State Key Laboratory of Disaster Reduction in Civil Engineering, Tongji University, Shanghai, China*
[2]*College of Civil Engineering, Tongji University, Shanghai, China*

(Received January 7, 2016, Revised November 13, 2017, Accepted November 13, 2017)

Abstract. High Damping Rubber bearings (HDR bearings) have been used in the seismic design of bridge structures widely in China. In earthquakes, structural natural periods will be extended, seismic energy will be dissipated by this kind of bearing. Previously, cyclic loading method was used mainly for test studies on mechanical properties of HDR bearings, which cannot simulate real seismic responses. In this paper, Real-Time Substructure (RTS) test study on mechanical properties of HDR bearings was conducted and it was found that the loading rate effect was not negligible. Then the influence of peak acceleration of ground motion was studied. At last test results were compared with a numerical simulation in the OpenSees software framework with the Kikuchi model. It is found that the Kikuchi model can simulate real mechanical properties of HDR bearings in earthquakes accurately.

Keywords: high damping rubber bearing; real-time substructure test; loading rate; numerical simulation

1. Introduction

High Damping Rubber bearing (HDR bearing) has been used in the seismic design of bridge structures widely in China, such as in the Hong Kong-Zhuhai-Macao Bridge. Advangtages of HDR bearings are the large vertical stiffness, small lateral stiffness and good energy dissipation capacity. In earthquakes, structural natural periods of bridges using HDR bearings are longer than those using fixed bearings, most seismic energy will be dissipated simultaneously and seismic forces will be reduced accordingly (Kelly 1991).

The rate-dependent behavior of high damping rubbers was investigated by the compression tests and a modified hyperelastic model was proposed by Amin *et al*. (2002) to represent the rate-independent elastic responses including the high initial stiffness feature. Material experiments necessary for modeling were systematically conducted and then a constitutive model for rubber materials was proposed by Yoshida *et al*. (2004). A new kind of anisotropic high damping rubber bearing was developed and studied by Burtscher and Dorfmann (2004), and the mechanical properties were studied by a series of compression and shear tests. The rate-dependent behavior of HDR bearings was also investigated by compression and shear tests by Amin *et al*. (2006a, b). The total stress was decomposed into an equilibrium stress and a viscosity-induced stress and an approach to extend the evolution equation for rate-dependent cyclic processes was proposed. Dall'Asta and Ragni (2006) conducted a series of compression and shear tests with different strain rates and strain amplitudes. A nonlinear viscoelastic damage model was proposed to describe the behaviour of rubber under cyclic loads. To study the influence of non-linear behaviour of HDR devices in the dynamic response of SDOF systems, Dall'Asta and Ragni (2008a, b) carried out preliminary analyses under harmonic forces and impulsive excitations. The mechanical behavior of HDR bearings was investigated under horizontal cyclic shear deformation with a constant vertical compressive load and an elasto-viscoplastic rheology model of HDR bearings for seismic analysis was developed by Bhuiyan *et al*. (2009).

Tubaldi *et al*. (2017) investigated the stress softening behaviour of HDR bearings and found that the differences between the quasi-static response and the other responses were very significant, confirming that the material should be modelled as a viscoplastic material (rather than an elasto-plastic material).

Previous test investigations of HDR bearings used mainly reversed cyclic loading method. In this paper Real-Time Substructure (RTS) test method was proposed to simulate the real-time seismic loading and introduced in detail at first. Then influences of loading rate and peak acceleration of ground motion were studied. Numerical simulation method was studied at last.

2. RTS test method

Seismic test methods were suggested to study mechanical properties of bearings in earthquakes. Among all the seismic test mothods, quasi-static test and pseudo dynamic test are loaded slowly and cannot take account of real loading rates (Leon and Deierlein 1996). Shake table test is loaded fast, but test specimens are usually scaled

*Corresponding author, Associate Professor
E-mail: ptb@tongji.edu.cn

Copyright © 2017 Techno-Press, Ltd.

ISSN: 2092-7614 (Print), 2092-7622 (Online)

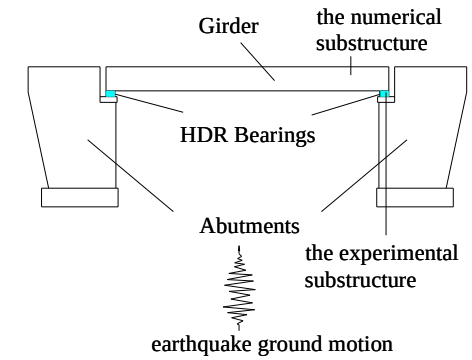

(a) A simply supported bridge

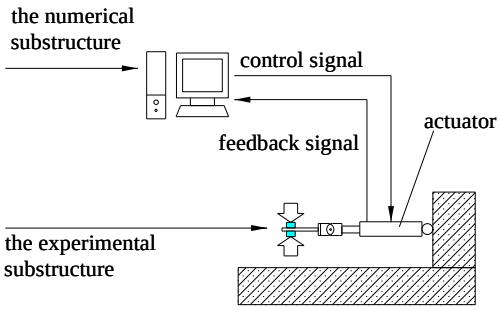

(b) Experimental and numerical substructures

Fig. 1 Schematic diagram of the RTS test method

down too much and cannot reflect real prototype properties (Tsai *et al*. 2007, Cheng 2008).

Therefore RTS test method was developed to overcome shortcomings mentioned above (Nakashima *et al*. 1992). It looks like a pseudodynamic test, but a time step of the test must be completed within a very small increment of time, so the test is loaded in real-time and test specimens are not necessary to be scaled down (Karavasilis *et al*. 2011, Asai *et al*. 2013, Wu *et al*. 2013).

In an RTS test, the researched structure would be divided into an experimental substructure and a numerical substructure using the substructure technique as in a pseudo-dynamic test. Usually the interested part of the structure or the part supposed to have significant nonlinear response under seismic loading is taken as an experimental substructure. And the remainder of the structure is taken as a numerical substructure and simulated in the computer. The interface actions between the two substructures are applied by actuators.

The RTS test method is introduced taking a simply supported bridge in Fig. 1(a) as an example. HDR bearings are selected as the experimental substructure and tested in parallel as shown in Fig. 1(b). The girder is selected as the numerical substructure and simulated in a computer.

The bridge in Fig. 1(a) can be simplified as an undamped single-degree of freedom (SDOF) system in Fig. 2. The structural damping is neglected for simplification. M stands for the girder mass, K stands for the nonlinear stiffness of the HDR bearing. The equation of motion of the system is

$$Ma_i + R_i = F_i \tag{1}$$

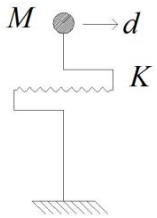

Fig. 2 A undamped single-degree of freedom system

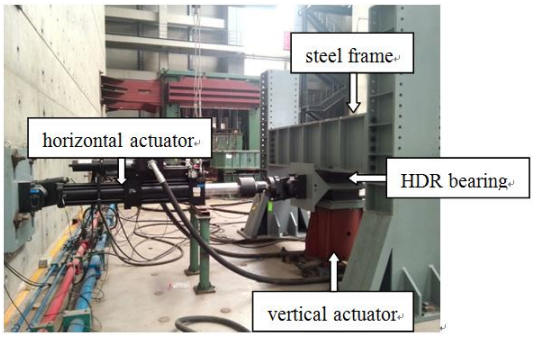

Fig. 3 RTS test setup

where, a and d stand for acceleration and displacement of the girder respectively. R stands for the bearing force measured currently and equals the product of K and the displacement. F stands for the seismic force at the time step. If Central Difference Method is used in the RTS test, the displacement command at the next time step is calculated with the following equation

$$d_{i+1} = 2d_i - d_{i-1} - \Delta t^2 \left(R_i - F_i \right) / M \tag{2}$$

The test procedure of the RTS test is as follows:

At t=0, set initial values of d, R and F to be zero.

1) According to Eq. (2), d_1 should be zero, and R_1 should be zero too.

2) At the first time step, namely t=Δt, the seismic force F_1 is input into the numerical substructure. d_2 can be calculated using Eq. (2).

3) d_2 is applied by the hydraulic servo actuator in a time step and the corresponding bearing force R_2 is measured and fed back to the numerical substructure.

4) d_3 can be calculated using Eq. (2) according to the current seismic force F_2.

5) Repeat step 4) and 5) until the end of the test.

3. RTS test setup

A series RTS tests were conducted in the state key laboratory of disaster reduction in civil engineering, Tongji University to study the mechanical properties of HDR bearings. RTS tests were conducted with the MTS FlexTest GT controller. The test setup was composed of a steel frame, a vertical actuator and a horizontal actuator, as shown in Fig. 3. The frame and vertical actuator were fixed on the ground and used to apply the vertical pressure on bearings. One end of the horizontal actuator was fixed on the reaction wall and the other end was connected to a

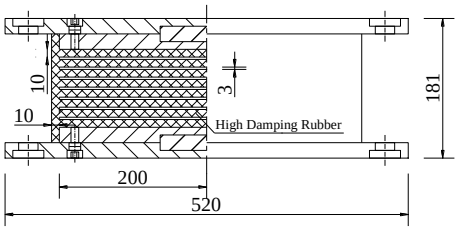

Fig. 4 Configuration of an HDR bearing (unit: mm)

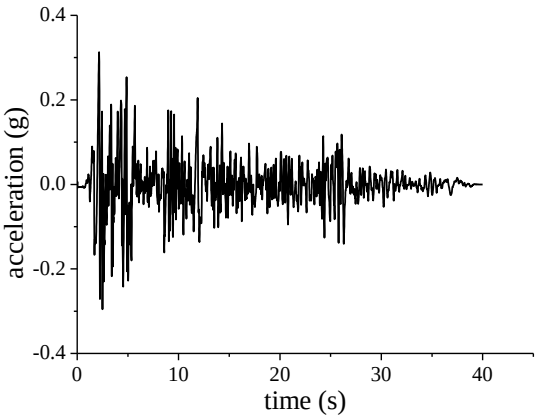

Fig. 5 El-Centro ground motion

loading plate which was inserted between the two bearings. The horizontal actuator was used to apply the horizontal displacement of bearings.

Each rubber layer of the HDR bearing is a square with side length 400 mm. The thickness of each rubber layer is 10 mm and that of each steel plate is 3 mm. The total thickness of rubber layers is 80 mm and that of the bearing is 181 mm. The configuration of an HDR bearing used in tests is shown in Fig. 4.

In RTS tests, El-Centro ground motion shown in Fig. 5 was input as the seismic acceleration time history. High damping rubber is an isotropic material, mechanical properties of HDR bearings in the longitudinal and transvers direction are the same, so only the longitudinal seismic responses of the bridge were analyzed for the sake of simplicity.

4. Influence of the loading rate

It is well known that loading rate has a great influence on mechanical properties of HDR bearings. However limited by the loading capacity, previous test studies on HDR bearings used mainly slowly loading method. If an RTS test is loaded slowly, it is degraded into a pseudo dynamic test. The difference between an RTS test and a pseudo dynamic test is the loading rate.

Suppose that the time step of an earthquake record is Δt and the loading time step, that is the duration to measure the bearing force, calculate the corresponding displacement and drive the actuator to the required position, is Δt_l. If $\Delta t_l=\Delta t$, the test will finish at the end of the earthquake record and it is so called a real time test. If $\Delta t_l>\Delta t$, the test will finish after the end of the earthquake record and it is so called a slow test. The longer the loading time step is, the slower the loading rate is. For example $\Delta t_l=n\Delta t$ and $n>1$, and then the loading rate of the slow test is n times slower than a real time test.

Table 1 Cases to study the influence of the loading rate

Case	1-1	1-2	1-3	1-4	1-5	1-6	1-7	1-8
Δt_l (s)	0.01	0.02	0.025	0.05	0.1	0.2	0.5	1.0
a_g (g)	0.2							
M (ton)	200							
N (kN)	960							

Table 2 Peak bearing responses for different loading rates

Case	Displacement (mm)			Force (kN)			Horizontal equivalent stiffness (kN/mm)
	max	min	Peak-to-peak	max	min	Peak-to-peak	
1-1	54.31	-57.93	112.24	177.12	-180.08	357.2	3.18
1-2	54.28	-56.16	110.44	157.04	-166.67	323.71	2.93
1-3	55.42	-58.21	113.63	156.24	-165.19	321.43	2.83
1-4	59.52	-60.57	120.09	159.67	-161.21	320.88	2.67
1-5	64.48	-63.39	127.87	163.87	-161.26	325.13	2.54
1-6	69.26	-65.78	135.04	167.27	-161.34	328.61	2.43
1-7	79.77	-64.78	144.55	178.53	-138.79	317.32	2.20
1-8	81.72	-64.20	145.92	177.37	-132.23	309.6	2.12

To study the influence of the loading rate, eight cases were arranged and listed in Table 1. In the table, Δt_l was the loading time step, a_g was the peak acceleration of El-Centro ground motion, M was the girder mass and N was the vertical pressure of the bearing. In the numerical substructure of this test, Δt was 0.01s, so only the case with a loading time step of 0.01s was a real time test. Other cases were all slow tests.

The bearing displacement time histories and hysteresis loops for different loading rates are shown in Fig. 6. The minimum and maximum bearing forces $F_{\min}$ and $F_{\max}$, minimum and maximum bearing displacements $d_{\min}$ and $d_{\max}$ for different loading rates are listed in Table 2. The horizontal equivalent stiffness is calculated according to the following equation.

$$K_{eq}=\left(F_{\max}-F_{\min}\right)/\left(d_{\max}-d_{\min}\right) \tag{3}$$

As shown in Fig. 6, the hysteresis loops are full and show good energy dissipation capacities. As shown in Table 2, with the decrease of the loading rate, the peak-to-peak value of bearing displacement increases most linearly, and the displacement increases by more than 30 percent by comparing Case 1-1 and 1-8. However, the peak-to-peak value of bearing force decreases by almost 10% by comparing Case 1-1 and 1-2, but changes a little from Case 1-2 to Case 1-7, and decreases by almost 3% by comparing Case 1-7 and 1-8. The horizontal equivalent stiffness decreases by more than 44 percent by comparing Case 1-1 and 1-8, due both to the increase of strain amplitude and to the decrease of the strain rates.

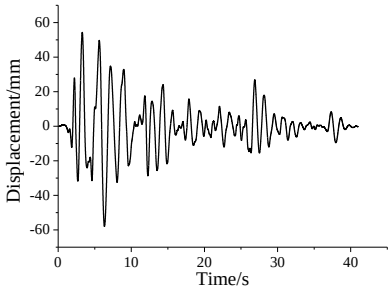

(a) Displacement time history for Δt_l=0.01s

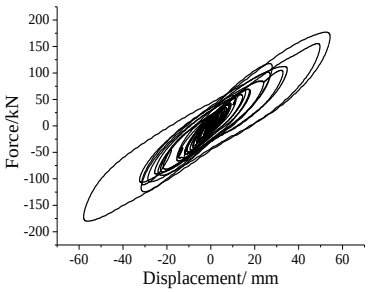

(b) Hysteresis loops for Δt_l=0.01s

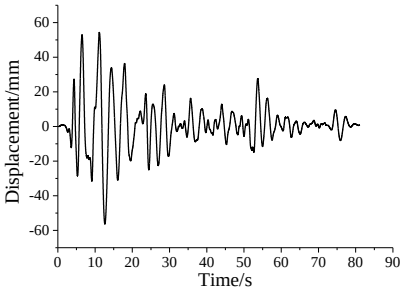

(c) Displacement time history for Δt_l=0.02s

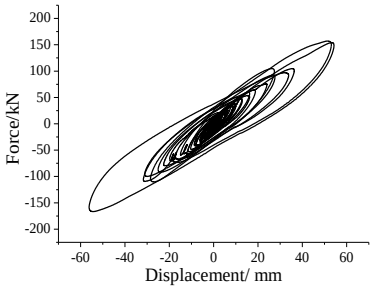

(d) Hysteresis loops for Δt_l=0.02s

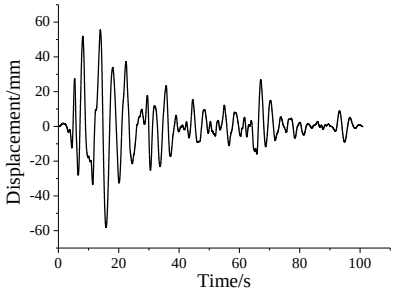

(e) Displacement time history for Δt_l=0.025s

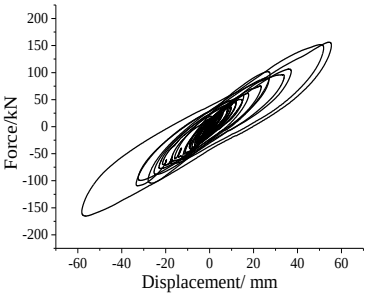

(f) Hysteresis loops for Δt_l=0.025s

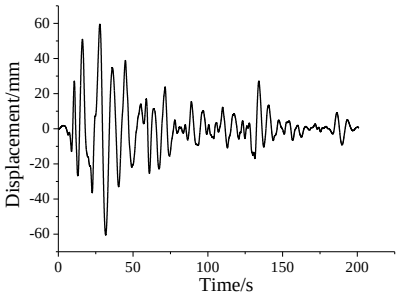

(g) Displacement time history for Δt_l=0.05s

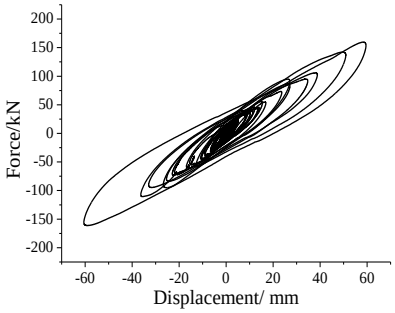

(h) Hysteresis loops for Δt_l=0.05s

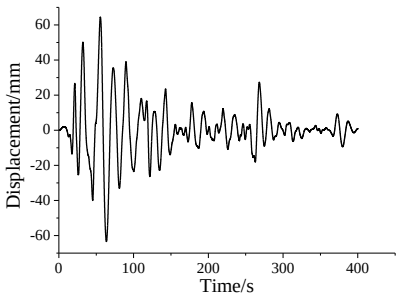

(i) Displacement time history for Δt_l=0.1s

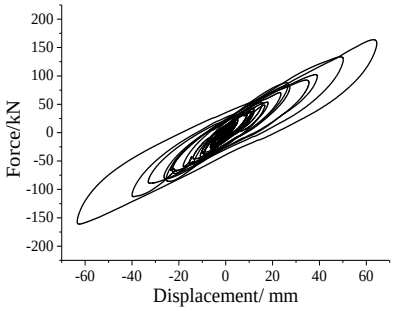

(j) Hysteresis loops for Δt_l=0.1s

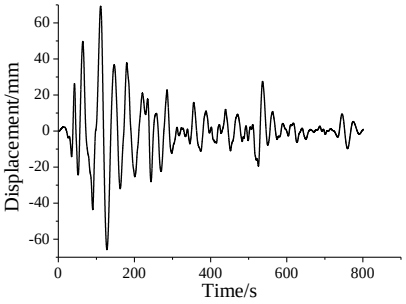

(k) Displacement time history for Δt_l=0.2s

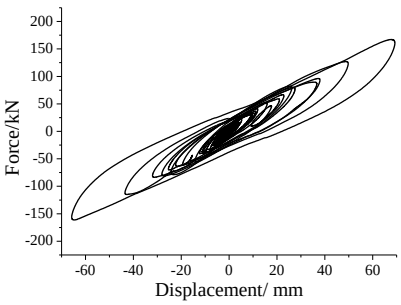

(l) Hysteresis loops for Δt_l=0.2s

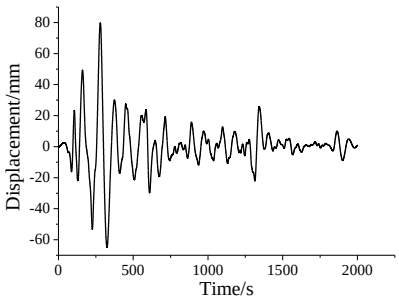

(m) Displacement time history for Δt_l=0.5s

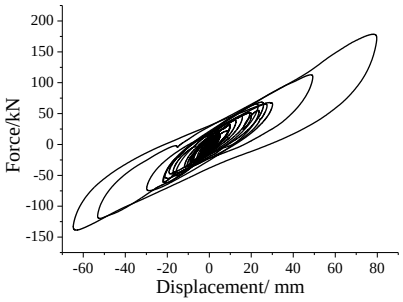

(n) Hysteresis loops for Δt_l=0.5s

Fig. 6 Test results for different loading rates

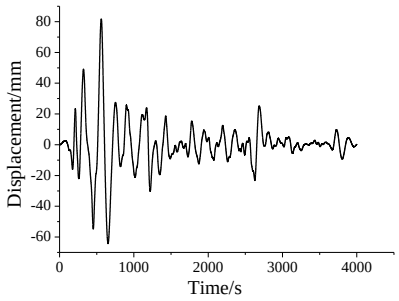

(o) Displacement time history for Δt_l=1.0s

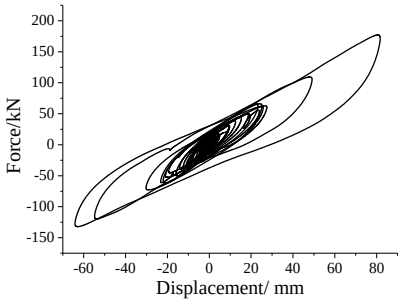

(p) Hysteresis loops for Δt_l=1.0s

Fig. 6 Continued

Table 3 Cases to study the influence of the peak acceleration

Case	2-1	2-2	2-3	2-4
Δt_l (s)				0.01
a_g (g)	0.1	0.15	0.2	0.25
M (ton)			200	
N (kN)			960	

Table 4 Peak bearing responses for different loading rates

Case	Displacement (mm)			Force (kN)			Horizontal equivalent stiffness (kN/mm)
	max	min	Peak-to-peak	max	min	Peak-to-peak	
2-1	28.21	-25.27	53.48	114.21	-103.88	218.09	4.08
2-2	41.53	-40.55	82.08	146.88	-138.87	285.75	3.48
2-3	54.31	-57.93	112.24	177.12	-180.08	357.20	3.18
2-4	68.93	-76.59	145.52	204.78	-236.43	441.21	3.03

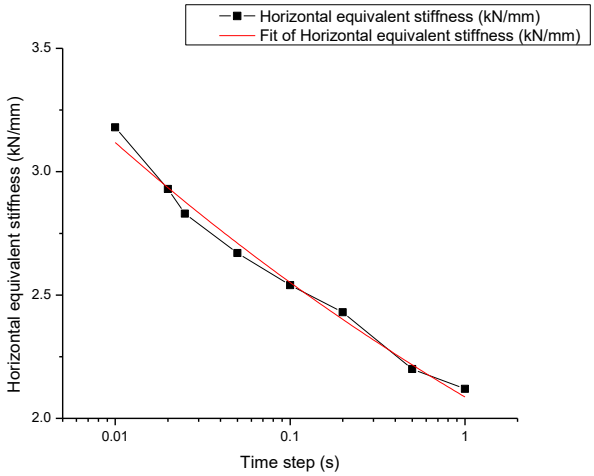

Fig. 7 The relationship between horizontal equivalent stiffness and time step

The relationship between horizontal equivalent stiffnesses and time steps is shown in Fig. 7. The relationship can be expressed by a simple equation with reasonable accuracy. The adjusted coefficient of determination is 0.98721.

$$K_{eq} = 2.08683 \times \left(\Delta t_l\right)^{-0.08722} \tag{4}$$

Slow test cannot take account of the loading rate effect and will greatly underestimate the real horizontal stiffness. To obtain the true seismic responses, a real time loading test method is necessary and the necessity of RTS tests is proven.

5. Influence of the peak acceleration

HDR bearing can be looked as a displacement-dependent device. Mechanical properties of HDR bearings would be influenced by bearing displacements. To study the influence of the bearing displacement, the peak acceleration of the ground motion was changed and four cases were arranged and listed in Table 3. The bearing displacement time histories and hysteresis loops for different peak accelerations are shown in Fig. 8. Peak bearing displacements and forces for different peak accelerations are listed in Table 4.

As shown in Fig. 8 and Table 4, with the increase of the peak acceleration, both bearing displacement and bearing force will increase. However, the horizontal equivalent stiffness decreases by more than 25%. So the influence of the peak acceleration on the horizontal equivalent stiffness is not negligible and an accurate numerical simulation method is necessary to estimate seismic responses of HDR bearings.

6. Numerical simulation

In current seismic design standards, HDR bearings are usually suggested to be simulated with bi-linear models (Ministry of Communications People's Republic of China 2008). However as shown above, HDR bearings contain quite complex hysteretic behaviors, which cannot be represented accurately by such a simple model. For seismic response analyses of structures supported and isolated by HDR bearings, an accurate model is necessary to characterize the hysteretic laws correctly. Several numerical models currently used in seismic applications for HDR bearings are rate-independent, and they are able to simulate mechanical properties of HDR bearings accurately (Kikuchi and Aiken 1997, Abe *et al*. 2004, Grant *et al*. 2004).

In the OpenSees software framework, a Kikuchi Bearing Element hysteresis model for HDR bearings and a uniaxial KikuchiAikenHDR material model were developed. The Kikuchi Bearing Element is a rate-independent model, but that can be used for seismic applications as shown below.

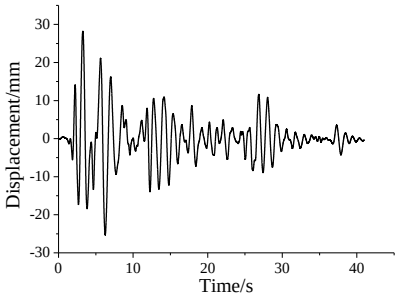

(a) Displacement time history for a_g=0.1 g

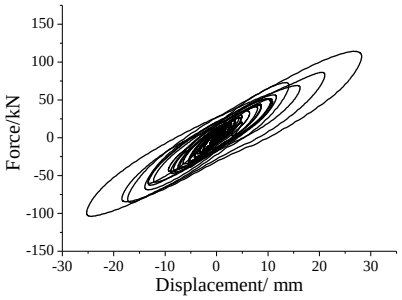

(b) Hysteresis loops for a_g=0.1 g

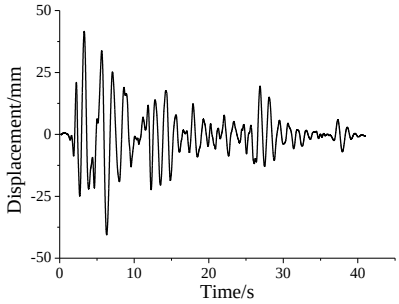

(c) Displacement time history for a_g=0.15 g

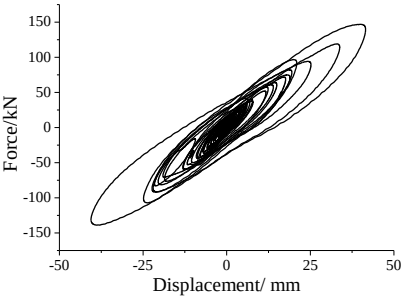

(d) Hysteresis loops for a_g=0.15 g

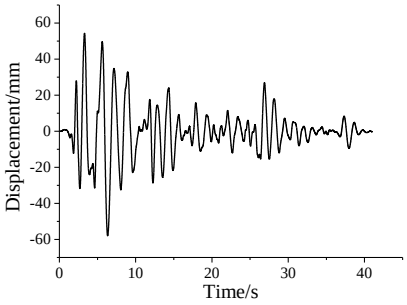

(e) Displacement time history for a_g=0.2 g

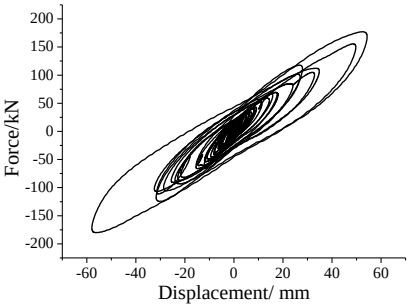

(f) Hysteresis loops for a_g=0.2 g

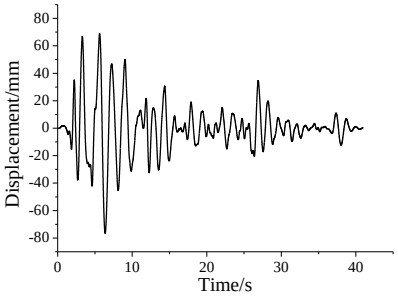

(g) Displacement time history for a_g=0.25 g

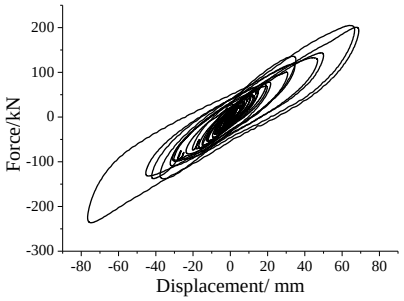

(h) Hysteresis loops for a_g=0.25 g

Fig. 8 Test results for different peak accelerations

It's proven that by considering different strain rates in the field of interest of seismic applications, the dependence on the strain rate is low and can be disregarded in numerical simulations (Aiken *et al*. 1992, Kikuchi and Aiken 1997). The model is defined by two nodes and consists of multiple shear spring model and multiple normal spring model and capable of well-predicting the mechanical properties of HDR bearings. In the KikuchiAikenHDR material model, three correction coefficients, i.e., *cg*, *ch*, *cu* for equivalent shear modulus, equivalent damping ratio, ratio of shear force at zero displacement respectively should be determined with the following equations.

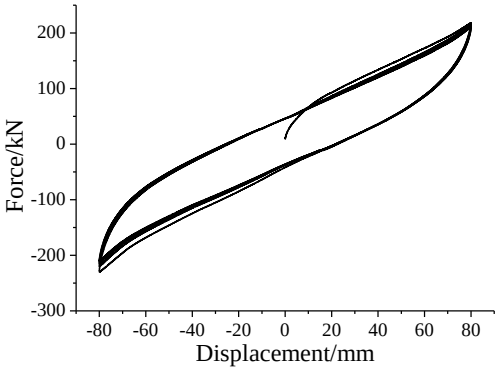

Fig. 9 Test hysteresis loops of the HDR bearing

Table 5 Comparisons of peak responses

Case		Test		Analysis		Error	
		Displacement (mm)	Force (kN)	Displacement (mm)	Force (kN)	Displacement (mm)	Force (kN)
3-1	max	28.21	114.21	27.70	112.19	-1.81%	-1.77%
	min	-25.27	-103.88	-22.86	-96.86	-9.54%	-6.76%
3-2	max	41.53	146.88	41.23	142.45	-0.72%	-3.02%
	min	-40.55	-138.87	-39.15	-136.80	-3.45%	-1.49%
3-3	max	54.31	177.12	54.39	168.25	0.15%	-5.01%
	min	-57.93	-180.08	-56.00	-171.22	-3.33%	-4.92%
3-4	max	68.93	204.78	66.13	189.20	-4.06%	-7.61%
	min	-76.59	-236.43	-76.89	-207.13	0.39%	-12.39%

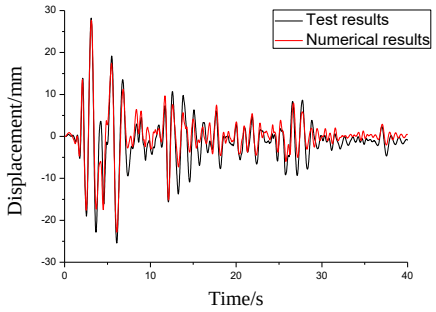

(a) Displacement time history for a_g=0.1 g

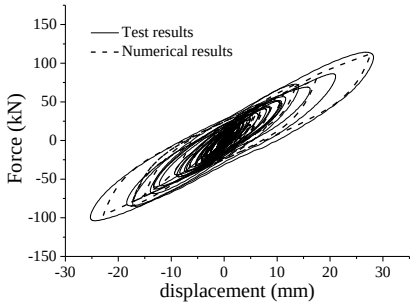

(b) Hysteresis loops for a_g=0.1 g

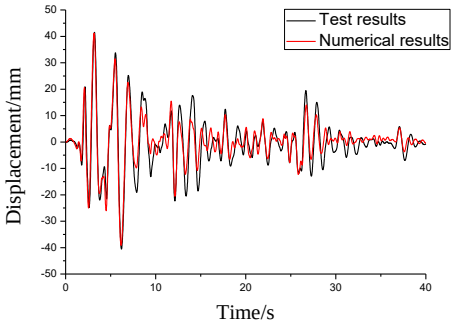

(c) Displacement time history for a_g=0.15 g

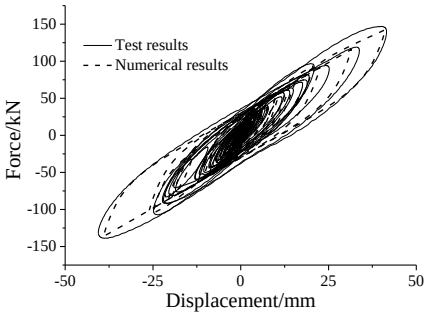

(d) Hysteresis loops for a_g=0.15 g

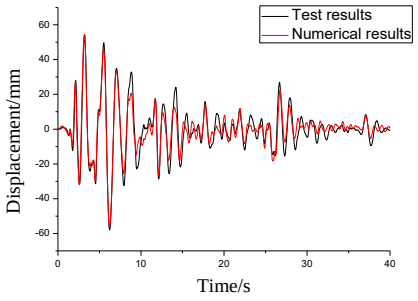

(e) Displacement time history for a_g=0.2 g

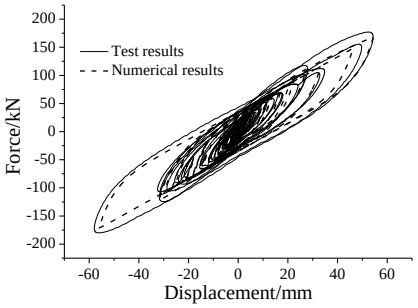

(f) Hysteresis loops for a_g=0.2 g

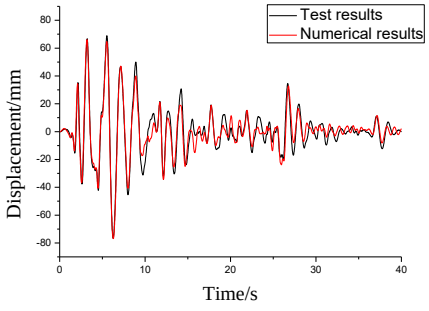

(g) Displacement time history for a_g=0.25 g

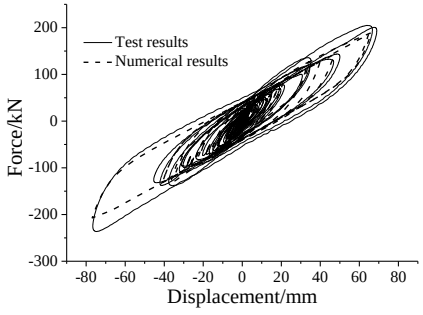

(h) Hysteresis loops for a_g=0.25 g

Fig. 10 Comparisons of test and analytical results for different peak accelerations

$$cg = \frac{G_{eq1}(\gamma)}{G_{eq2}(\gamma)} = \frac{G_{eq1}(\gamma)\frac{A}{T_r}}{G_{eq2}(\gamma)\frac{A}{T_r}} = \frac{K_{eq1}(\gamma)}{K_{eq2}(\gamma)} \quad (5)$$

$$ch = \frac{\xi_{eq1}(\gamma)}{\xi_{eq2}(\gamma)} \quad (6)$$

$$cu = \frac{u_1(\gamma)}{u_2(\gamma)} \quad (7)$$

$G_{eq1}(\gamma)$, $K_{eq1}(\gamma)$, $\xi_{eq1}(\gamma)$, $u_1(\gamma)$ are the equivalent shear modulus, equivalent horizontal stiffness, equivalent damping ratio, ratio of shear force at zero displacement obtained from a cyclic loading test with loading frequency of 1 Hz. The test was conducted using the specimen shown in Fig. 4 with the maximum shear strain of 100%. The test hysteresis loops of the HDR bearing are shown in Fig. 9 and $K_{eq1}(\gamma)$, $\xi_{eq1}(\gamma)$, $u_1(\gamma)$ are 2.65 kN/mm, 0.1141, 0.19 respectively.

$G_{eq2}(\gamma)$, $K_{eq2}(\gamma)$, $\xi_{eq2}(\gamma)$, $u_2(\gamma)$ are those obtained from a numerical analysis with the same maximum shear strain and the correction coefficients are set to be 1. According to the test and analytical results, *cg*, *ch*, *cu* are 1.94, 0.54, 0.52 respectively.

In order to verify the feasibility of simulating mechanical properties of HDR bearings with the Kikuchi Bearing Element, RTS test results of the four cases in section 5 and numerical analysis are compared. A numerical analysis is conducted with the model shown in Fig. 2. In the numerical analysis, a model with the same structural and earthquake parameters as in section 5 is established.

Test and numerical results for the model are presented in Table 5 and Fig. 10. Table 5 summarizes the test and analytical peak responses, listing peak bearing displacements and forces, and the error between the test and analytical results. Analytical peak response quantities are all within 15 per cent of the test values.

Fig. 10 presents comparisons of the time histories and hysteresis loops for the El Centro input. Analytical displacement time histories show good agreement with the test results as shown. Correlation coefficients of bearing displacement histories for the four cases between test and numerical results are 91.71%, 91.40%, 94.87% and 95.94% respectively.

As shown in hysteresis loops for the four cases, bearing forces of analytical results are all less than those of test results. The max error is more than 10%. Therefore, the bearing force is underestimated with the Kikuchi Bearing Element although the bearing displacement is simulated very well. The numerical simulation method includes the following steps:

1) Conducting a low-frequency cyclic loading test with the maximum shear strain of 100%.

2) Caluculating $K_{eq1}(\gamma)$, $\xi_{eq1}(\gamma)$, $u_1(\gamma)$ according to the test results.

3) Caluculating $K_{eq2}(\gamma)$, $\xi_{eq2}(\gamma)$, $u_2(\gamma)$ according to a numerical analysis with the maximum shear strain of 100% and the correction coefficients are set to be 1.

4) Caluculating cg, ch, cu according to Eqs. (5)-(7).

5) Establishing a numerical structural analysis model in the OpenSees software framework, where HDR bearings are modeled by the Kikuchi Bearing Element.

7. Conclusions

Mechanical properties of HDR bearings are studied using the RTS test method, and a simulation method with the Kikuchi Bearing Element is suggested. The following conclusions can be drawn:

1) The loading rate effect of HDR bearings should be paid full attention and a real-time loading test method such as RTS test method is necessary to obtain the real seismic responses. However, the loading rate effect is not significant in the rage of strain-rates of interest in seismic applications.

2) The influence of peak accelerations is not negligible and should be considered adequately.

3) The Kikuchi Bearing Element in the OpenSees software framework can simulate mechanical properties of HDR bearings with acceptable accuracy. The bearing displacement is simulated very well, however, the bearing force is underestimated a little.

Acknowledgments

This work was supported in part by the National Natural Science Foundation of China (No. 51278372) and the Ministry of Science and Technology of China, Grant No. SLDRCE 14-B-15.

References

Abe, M., Yoshida, J. and Fujino, Y. (2004), "Multiaxial behaviours of laminated rubber bearings and their modeling. II: modelling", *J. Struct. Eng.*, **130**(8), 1133-1144.

Aiken, I.D., Kelly, J.M., Clark, P.W., Tamura, K., Kikuchi, M. and Itoh, T. (1992), "Experimental studies of the mechanical characteristics of three types of seismic isolation bearings", *Proceedings of The 10th World Conference on Earthquake Engineering*, Vol. 4, Madrid, 2281-2286.

Amin, A.F.M.S., Alam, M.S. and Okui, Y. (2002), "An improved hyperelasticity relation in modeling viscoelasticity response of natural and high damping rubbers in compression: experiments, parameter identification and numerical verification", *Mech. Mater.*, **34**(2), 75-95.

Amin, A.F.M.S., Wiraguna, S.I., Bhuiyan, A.R. and Okui, Y. (2006), "Hyperelasticity model for FE analysis of natural and high damping rubbers in compression and shear", *J. Eng. Mech.*, ASCE, **132**(1), 54-64.

Amin, A.F.M.S., Lion, A., Sekita, S. and Okui, Y. (2006), "Nonlinear dependence of viscosity in modeling the rate-dependent response of natural and high damping rubbers in compression and shear: Experimental identification and numerical verification", *Int. J. Plasticity*, **22**(9), 1610-1657.

Asai, T., Chang, C.M. and Phillips, B.M. (2013), "Real-time hybrid simulation of a smart outrigger damping system for high-rise buildings", *Eng. Struct.*, **57**, 177-188.

Bhuiyan, A.R., Okui, Y., Mitamura, H. and Imai, T. (2009), "A rheology model of high damping rubber bearings for seismic analysis: Identification of nonlinear viscosity", *Int. J. Solid. Struct*., **46**(7-8), 1778-1792.

Burtscher, S.L. and Dorfmann, A. (2004), "Compression and shear tests of anisotropic high damping rubber bearings", *Eng. Struct*., **26**(13), 1979-1991.

Cheng, C.T. (2008), "Shaking table tests of a self-centering designed bridge substructure", *Eng. Struct*., **30**(12), 3426-3433.

Dall'Asta, A. and Ragni, L. (2006), "Experimental tests and analytical model of high damping rubber dissipating devices", *Eng. Struct*., **28**(13), 1874-1884.

Dall'Asta, A. and Ragni, L. (2008), "Nonlinear behavior of dynamic systems with high damping rubber devices", *Eng. Struct*., **30**(12), 3610-3618.

Dall'Asta, A. and Ragni, L. (2008), "Dynamic systems with high damping rubber: nonlinear behaviour and linear approximation", *Earthq. Eng. Struct. Dyn*., **37**(13), 1511-1526.

Grant, D.N., Fenves, G.L. and Whittaker, A.S. (2004), "Bidirectional modeling of high-damping rubber bearings", *J. Earthq. Eng*., **8**(1), 161-185.

Karavasilis, T.L., Ricles, James M., Sause, R. and Chen, C. (2011), "Experimental evaluation of the seismic performance of steel MRFs with compressed elastomer dampers using large-scale real-time hybrid simulation", *Eng. Struct*., **33**(6), 1859-1869.

Kelly, J.M. (1991), *Dynamic and Failure Characteristics of Bridgestone Isolation Bearings*, Research Report No. UCB/EERC-91/04; Earthquake Engineering Research Center, The University of California at Berkeley, USA.

Kikuchi, M. and Aiken, I.D. (1997), "An analytical hysteresis model for elastomeric seismic isolation bearings", *Earthq. Eng. Struct. Dyn*., **26**(2), 215-231.

Leon, R.T. and Deierlein, G.G. (1996), "Consideration for the use of Quasi-Static test", *Earthq. Spec*., **12**(1), 87-109.

Ministry of Communications People's Republic of China (2008), Guidelines for seismic design of highway bridges, JTG/TB 02-01-2008, People's Communications Publishing House, Beijing, China.

Nakashima, M., Kato, H. and Takaoka, E. (1992), "Development of real-time pseudo dynamic testing", *Earthq. Eng. Struct. Dyn*., **21**(1), 79-92.

Tubaldi, E., Ragni, L., Dall'Asta, A., Ahmadi, H. and Muhr, A. (2017), "Stress softening behaviour of HDNR bearings: modelling and influence on the seismic response of isolated structures", *Earthq. Eng. Struct. Dyn*., **46**(12), 2033-2054.

Tsai, M.H., Wu, S.Y. and Chang, K.C. (2007), "Shaking table tests of a scaled bridge model with rolling-type seismic isolation bearings", *Eng. Struct*., **29**(5), 694-702.

Wu, B., Wang, Z. and Bursi, O.S. (2013), "Actuator dynamics compensation based on upper bound delay for real-time hybrid simulation", *Earthq. Eng. Struct. Dyn*., **42**(12), 1749-1765.

Yoshida, J., Abe, M. and Fujino, Y. (2004), "Constitutive modeling for high-damping rubber materials", *J. Eng. Mech*., ASCE, **130**(2), 129-141.

CC